4A.6 SUMMERTIME OCEANIC FLUXES AT SHEBA: OBSERVATIONS AND STEADY 2-D MODELLING

Daniel R. Hayes*, J. H. Morison, M. G. McPhee
Applied Physics Laboratory
University of Washington, Seattle, Washington

1. **INTRODUCTION**

The surface heat budget of the Arctic Ocean plays an important part in the evolution of the ice cover. In turn, the ice cover affects the surface heat and salt budgets by acting as a source or sink of fresh water and as a good insulator and reflector of radiation relative to open water. In summer, fresh or brackish water enters the ocean from basal melting and from surface melting via leads and percolation through the ice. Meanwhile, solar heating in leads is strong, and wind and ice motion stir the upper ocean. The oceanic boundary layer is the site where the surface heat, salt and momentum fluxes interact with each other and with the ice.

Our goal is to improve the understanding of the oceanic boundary layer in order to pin down the partitioning of incoming solar radiation in the Arctic to basal melting, lateral melting, storage in the mixed layer, and loss to the atmosphere. To this end, we investigate internal boundary layer development under horizontally varying surface stress, radiative forcing, and surface buoyancy flux. Data from the Surface HEat Balance of the Arctic Ocean (SHEBA) from the summer of 1998 as well as two-dimensional steady boundary layer modelling inform this study.

*_Corresponding author address:_ Daniel R. Hayes, Applied Physics Laboratory, 1013 NE 40th St., Seattle, WA 98105; email: dhayes@apl.washington.edu

2. **OBSERVATIONS**

Horizontal profiles of temperature, conductivity, and deviations of vertical velocity were gathered in and around a lead at the SHEBA site during July and August of 1998. The temperature and conductivity data were collected by probes on the Autonomous Micro-conductivity Temperature Vehicle (AMTV), and the vertical water velocity was calculated from vehicle depth, pitch, and pitch rate using a Kalman smoothing algorithm. The instrument and smoothing technique are described in detail by Hayes and Morison (submitted in 2000). These unique observations show horizontal snapshots of the boundary layer at multiple depths, including vertical heat and salt fluxes and vertical velocity, mixing length, and surface roughness.

The study began with a calm, mostly sunny period during mid-July in which meltwater filled the lead and eventually extended below the mean ice thickness. In late July, the wind stress increased enough to mix down the fresher, warmer layer and also opened the lead substantially. After the fresh layer was depleted in early August, wind and ice motion continued to mix down the fresh, warm meltwater input. Under the lead, the heat flux and fresh water flux measured by the AMTV were both strongly downward, while under the ice, the heat and salt fluxes were small and often indistinguishable from zero. This is illustrated by Figure 1 which shows data from late in day 7 August 1998. For this segment, the AMTV was swimming at about five

meters depth. The temperature rises slowly as the downstream edge of the lead is approached from upstream, consistent with continuous solar heating and vertical mixing of warmer surface water as water traverses the lead. The salinity drops steadily in conjunction with the temperature rise, also indicating continuous mixing down of freshwater input at the upstream side of the lead. The vertical velocity fluctuations suggest that about 100 m downstream of the lead edge, the turbulent vertical water velocity jumps in total energy and in characteristic wavelength. The fluxes in the lead indicate warm, fresh water moving downward, while under the ice, fluxes are quite small. Figure 1 paints a picture of a steady-state internal boundary layer whose structure is determined by the surface boundary conditions. Fresh, warm water is mixed downward in the lead by wind stress; the turbulence is stabilized by the buoyancy flux. Under the ice, fluxes are small, and the characteristic turbulent length scale and turbulent energy increase. The next step is to determine the fate of the heat flux below five meters in the lead. Since the data are limited in extent for both time and space, a numerical model has been used.

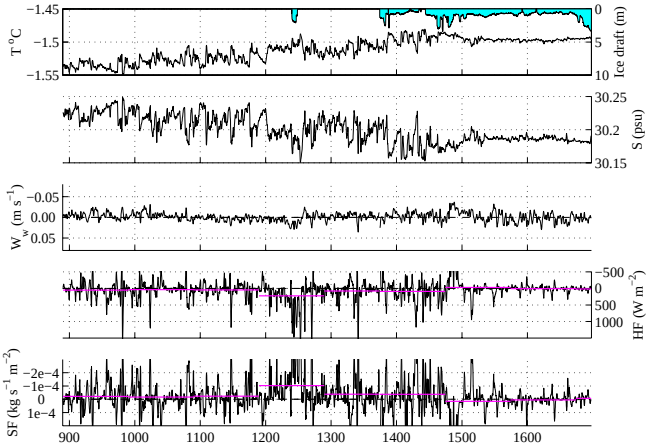

FIGURE 1. AMTV data from run 2 of SHEBA on 7 August 1998 (0000 UT 8 August). Vehicle speed was 1.1 m s^{-1}, and depth was five meters. Ice draft is shown and ice velocity is from right to left at 0.15 m s^{-1}. Mean fluxes are indicated by the solid lines. In the lead the heat flux is -69 W m^{-2} (downward), and the salt flux is 3.0x10^{-5} kg s^{-1} m^{-2} (upward). Correlation coefficients between temperature or salinity and water velocity are significant at the 99% level under the lead and are insignificant under the ice. The x-axis is distance in meters.

3. **MODELLING**

A boundary layer model adapted from McPhee (1987, 1992) is used to simulate conditions like those on 7 August 1998 at SHEBA. In its original form, it is a one-dimensional, time-dependent, horizontally homogeneous, first order closure model. Geostrophic velocity and mean vertical velocity are assumed zero. The model eddy viscosity is calculated as the product of a characteristic eddy overturning velocity and an eddy mixing scale (the mixing length). The mixing length is in calculated based on distance from the ice, stratification, buoyancy flux, and surface stress. Boundary conditions at the surface are heat, salt, and momentum flux and surface roughness, which can all vary in time. The ice-ocean fluxes are determined using the bulk heat transfer model of *McPhee* (1992). The model solutions are transformed from temporal to spatial using the mean ice velocity. In this way, the model is essentially a steady, but 2-D (x-z) model.

A simulation of the lead at SHEBA on 7 August 1998 is shown in Figure 2. The lead is modelled by a 1.25 km segment with incoming shortwave radiation of 448 W m^{-2} (courtesy of the SHEBA Project Office), a surface friction velocity of 0.8 x 10^{-3} m s^{-1}, a roughness length of 2.7 x 10^{-5} m, and no surface melting. The surface stress and roughness

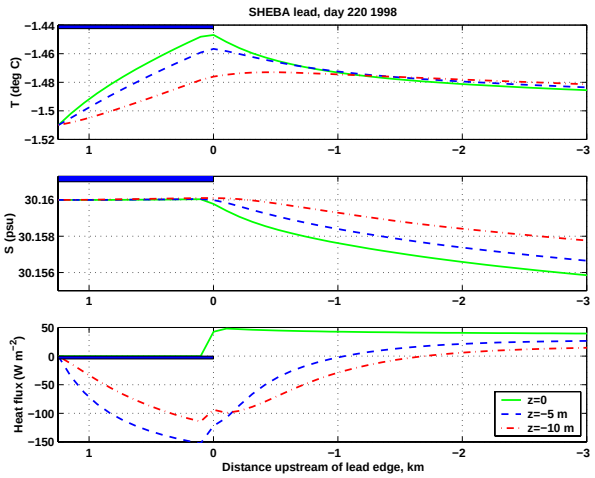

FIGURE 2. Simulation of 1.25 km lead under conditons similar to that of Figure 1. The solid bar on the left indicates the lead, which has an incoming shortwave radiative flux of 448 W m^{-2} and an albedo of 0.08. The ice is moving from right to left at 0.17 m s^{-1}. Horizontal profiles are taken at 0, 5, and 10 meters.

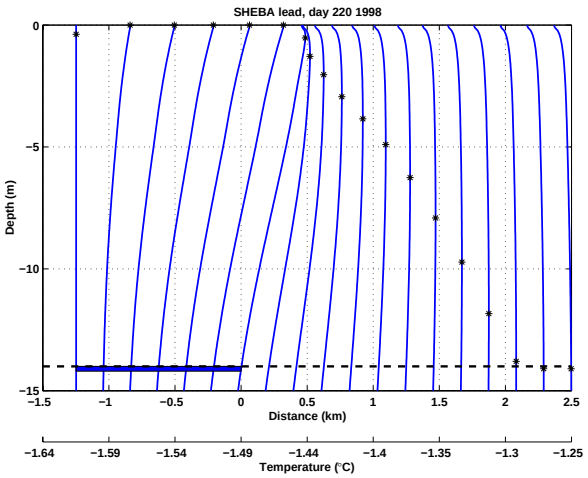

FIGURE 3. Temperature profiles for the lead simulation of Figure 2. The thick line represents the lead, and the base of each profile is positioned at the correct location. Temperature maxima are indicated by the asterisks.

---

lengths were calculated using the 10-m wind speed and equations from Steele et al. (1989). The ice boundary conditions downstream of the lead change to allow melting, the radiative flux stops, and surface friction velocity and roughness length increase to 0.01 m s^{-1} and 0.01 m, calculated from ice velocity using a Rossby similarity law and an educated guess, respectively. The initial temperature and salinity profiles mimic those observed on 7 August: a 20-meter mixed layer with salinity of 30.16 psu and temperature of -1.51 ^{o}C, more than 0.1 C^{o} above the freezing temperature. A constant-N^2 (1.3x10^{-3} s^{-1}) pycnocline is set below 20 m.

Results show that, like the AMTV data, temperature increases steadily as the downstream lead edge is approached, and fall or level off under the ice. Again, this is consistent with the continuous solar heating and mixing down of the surface water. However, the salinity does not decrease in the lead, as the data indicates, but under the ice. This can be explained by the lack of a surface fresh water source in the model lead that will be added in the future. It will be necessary to estimate the amount of fresh water that is draining into the lead from the ice edges, as well as the amount percolating through the ice. Currently in the model, the only fresh water source is the melting caused by the ocean above its freezing point. It should be noted that the salinity decrease in the model is very small and would not be detectable in Figure 1.

It is interesting to note that the heat flux under the lead is more negative at five meters than at 10 meters, yet about 1 km downstream of the lead, the flux at five meters goes upward, while the flux at 10 m remains downward until 2 km downstream. This helps explain why the fluxes measured by the AMTV at five meters under the ice are barely detectable only a short distance downstream of the lead. This can be more easily visualized by looking

at temperature profiles (Fig. 3). The temperature maxima are indicated by asterisks, above which the heat flux is upward, and below which the heat flux is downward.

The model is also used to investigate the horizontal dependence of the characteristic turbulent length scale (mixing length) and turbulent kinetic energy (Fig. 4). The friction velocity is used as a proxy for turbulent energy, and the plot shows that it increases under the ice, as expected since the surface friction velocity also increases under the ice. The mixing length, however, does not show much change except for a momentary decrease due to the fresh water input when melting begins. A realistic source of fresh water in the lead would reduce the mixing length at five meters under the lead relative to under the ice. Finally, the across-lead velocity is plotted in the third panel. This brings to light the limitations of the model because near the lead edge, the velocity changes rapidly, but the model assumes horizontal homogeneity, so it does not account for this horizontal convergence. The advective transformation from time to space is therefore questionable. The region between flow affected by the lead surface and by the ice surface may be of importance because it should be a zone of intensified turbulence.

4. **CONCLUSION**

The oceanic boundary layer in and around leads is an important piece of the surface heat budget puzzle. Further analysis of horizontal profiles of turbulent quantities gathered by the AMTV will help understand general features of the horizontally inhomogeneous boundary layer. Further modelling studies will also aid in explaining the effects of the

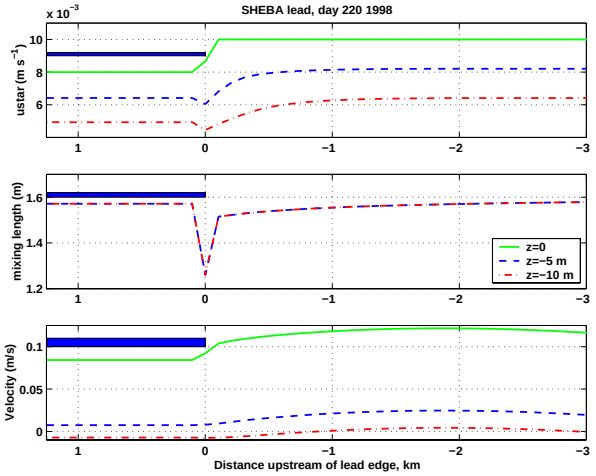

FIGURE 4. As in Figure 2, but for surface friction velocity, mixing length, and velocity.

boundary layer on the partitioning of incoming radiation to lateral and basal melt, and oceanic storage. The potential effects of the internal boundary layer will be investigated, although a higher dimensional model would be required to fully simulate the transition from lead to ice boundary conditions.

5. **REFERENCES**

Hayes, D.R., and J. H. Morison, 2000: Determining turbulent, vertical velocity and the fluxes of heat and salt in the polar ocean boundary layer with an autonomous underwater vehicle. submitted to *J. Atmos. and Oceanic Tech.*

McPhee, M. G., 1992: Turbulent heat flux in the upper ocean under sea ice. *J. Geophys. Res.*, **97**(C4), 5365-5379.

McPhee, M. G., 1987: A time-dependent model for turbulent transfer in a stratified oceanic boundary layer. *J. Geophys. Res.*, **92**(C7), 6977-6986.

Steele, M., J. H. Morison, and N. Untersteiner, 1989: The partition of air-ice-ocean momentum exchange as a function of ice concentration, floe size, and draft. *J. Geophys. Res.*, **94**(C9), 12,739-12,750.